



Structural and fluorescence properties of thin films fabricated by pulsed laser deposition technique from Nd:KGW single crystal

J. Lancok^{a,b,*}, C. Garapon^b, V. Vorlíček^a, M. Jelinek^a, M. Čerňanský^a

^a Institute of Physics ASCR, Na Slovance 2, 182 21 Prague 8, Czech Republic

^b Laboratoire de Physico-Chimie des Matériaux Luminescents, CNRS-Université Lyon-I, 10 rue Ampère, 69622 Villeurbanne Cedex, France

Received 16 July 2004; accepted 19 January 2005

Abstract

Textured and amorphous thin films were deposited by KrF laser ablation of neodymium doped potassium gadolinium tungstate, $\text{KGd}_{1-x}\text{Nd}_x(\text{WO}_4)_2$ (Nd:KGW) single crystal in oxygen ambient atmosphere on MgO, YAP (YAlO_3) and YAG ($\text{Y}_3\text{Al}_5\text{O}_{12}$) substrates at temperatures up to 800 °C. The influence of substrate nature and substrate temperature (T_s) on films crystallinity and morphology were studied by conventional X-ray diffraction (XRD), micro-Raman spectroscopy (μRS) and scanning electron microscopy (SEM). Related emission and excitation spectra and fluorescence decay were examined. The strongly textured polycrystalline Nd:KGW films with fluorescence spectra very close to those of bulk single crystal were deposited only on YAG substrate at higher T_s , whereas the smoother films were obtained at $T_s = 400$ °C on all types of substrates. Fluorescence properties of the films corresponding to the transitions from the $^4\text{F}_{3/2}$ doublet to the $^4\text{I}_{9/2}$, $^4\text{I}_{11/2}$ and $^4\text{I}_{13/2}$ multiplets, at about 890 nm, 1.06 μm and 1.3 μm , bring a new information about the structure of the film at the scale of the Nd^{3+} ions environment, which could not be detected by XRD method. The fluorescence decay was almost exponential, with a lifetime of about 110 μs for polycrystalline KGW films.
© 2005 Elsevier B.V. All rights reserved.

PACS: 42.70–Hj; 42.70–a; 81.15–Fg; 78.55–Hx

Keywords: Micro-Raman spectroscopy; Nd:KGW films

1. Introduction

Potassium gadolinium tungstate $\text{KGd}(\text{WO}_4)_2$, denoted as KGW, is known from the beginning of the 70th [1]. Nevertheless, it represents relatively new attractive laser host crystals. KGW doped with rare-earth ions attracts great interest as efficient low threshold solid-state laser material with interesting optical properties. Monoclinic low temperature phase denotes as α -KGW can be obtained only by a growth from the flux [2]

and crystallises in the monoclinic centrosymmetric space group $C2/c$ with lattice parameters $a = 10.65$ Å, $b = 10.37$ Å, $c = 7.58$ Å, and $\beta = 130.75^\circ$ [3]. More details about the KGW structural and optical properties can be found for example in [2–6]. In the last years, there have been many reports on laser and spectroscopic properties of KGW crystal doped with Nd^{3+} [4,6–8], Er^{3+} [5,9], Yb^{3+} [10,11], Ho^{3+} [12], Pr^{3+} [13,14], Dy^{3+} [2] and Tm^{3+} [15]. Among those especially Nd:KGW is intensively studied, because it has several additional advantages over the most usual Nd:YAG laser such as higher slope efficiency, better characteristic for diode pumping, higher doping level [8], up to 50 at.% can be achieved without changing the structure [16], and high third order nonlinear susceptibility $\chi^{(3)}$. More detail

* Corresponding author. Address: Institute of Physics ASCR, Na Slovance 2, 182 21 Prague 8, Czech Republic. Tel.: +420 266052645; fax: +420 286890527.

E-mail address: lancok@fzu.cz (J. Lancok).

about comparison of lasing properties of Nd³⁺ ions in KGW and YAG crystals can be found in [6,8,17]. However, there are also some drawbacks for wider application of the doped KGW in the laser technology. First, it is not easy to grow high quality crystals in large dimensions (usually up to 10 mm) and secondly, its thermomechanical properties are less favourable in comparison with YAG [6]. Nevertheless some of the optical characteristics of Nd:KGW such as high level doping and better optical characteristics for laser diode pumping make it an attractive candidate for compact high gain micro-laser systems [8]. So, in respect to the above mentioned advantages and drawbacks, Nd:KGW seems to be a very interesting material for thin planar waveguide laser application.

Pulsed laser deposition (PLD) is an attractive technique to elaborate materials in thin film form, and is specially suited for the deposition of oxide systems due to the possibility to transfer materials stoichiometry from the target to the substrate. By this method several high quality and low loss active waveguides have been grown such as Er:Y₂O₃ [18] and Nd:YAP [19] on sapphire substrates. Furthermore up to now laser operation has been demonstrated on Nd:GGG [20] and Ti:sapphire [21] waveguides made by this technique. **Recently studies about growing of Nd:KGW thin films on (1 1 0 2) sapphire [22,23], YAG [23] and Si [24] substrates by PLD have been published.** We have also reported results about the growth of Nd:KGW films [25] on different kind of substrates such as MgO, YAG, YAP and Si. All this study has shown a significant influence of

substrate nature on structural properties of elaborated films.

The aim of this contribution is to study the influence of the structure of the deposited films on their fluorescence properties more in detail than in previous published work.

2. Experimental

The preparation procedure was described more in detail in [25]. Briefly, a KrF excimer laser beam was focused on Nd:KGW target, so that an energy density of the laser beam on the target of 2 J cm⁻² was reached. Optically polished substrates, (100) MgO (cubic, $a = 4.21 \text{ \AA}$), (100) YAG (cubic, $a = 12.01 \text{ \AA}$) and (100) YAP (rhombic, $a = 5.17 \text{ \AA}$, $b = 5.31 \text{ \AA}$, $c = 7.35 \text{ \AA}$), were positioned 5 cm away from the target and mounted on a massive resistively heated holder. The substrates temperature T_S was varied between 400 °C and 800 °C. The deposition was carried out in oxygen ambient at 20 Pa. The film thickness, measured by mechanical profilometer TENCOR 500, varied from 400 nm to 1200 nm. The deposition parameters and some of the films properties are summarised in Table 1. After all measurements we tried to improved the crystalline structure of the amorphous films deposited at 400 °C (KGW3 and KGW10—see Table 1) by a thermal annealing in the argon atmosphere at 1000 °C for 1 h. To minimise a thermal stress, the temperature rise during the heating and cooling was 2 °C per minute.

Table 1
Summary of deposition conditions and of some properties of Nd:KGW films deposited by PLD

Sample	Substrate	T_S [°C]	Thickness [nm]	Crystallinity strongest reflection	Crystal dimension		Lifetime [μs]
					SEM [μm]	XRD [nm]	
KGW3	MgO	400	435	Amorphous	No cryst.	No cryst.	–
KGW3 Annealed	MgO	$T_{an} = 1000$	–	Polycrystalline (040) GdW Minority KGW	10 GdW 1–2 KGW	124 nm GdW 61 nm KGW	–
KGW4	MgO	501	410	Nearly amorphous	–	–	–
KGW5	MgO	606	420	Polycrystalline, (220) KGW, broad Minority GdW	~1	–	–
KGW6	MgO	700	450	Polycrystalline, (131) KGW, broad Minority GdW	–	–	–
KGW7	MgO	800	430	Polycrystalline, (040) GdW, broad Minority KGW	1–2	61 nm	~100
KGW9	YAG	700	1200	Polycrystalline, (221) KGW,	3–5	235 nm	110
KGW10	YAG	400	1160	Nearly amorphous	–	–	160
KGW10 Annealed	YAG	$T_{an} = 1000$	–	Polycrystalline (002) KGW	3–5	95 nm	–130 108
KGW11	YAP	400	1100	Amorphous	No cryst.	No cryst.	–
KGW8	YAP	700	1150	Polycrystalline, Small broad peaks	<1	–	–

The crystalline structure has been investigated by conventional XRD measurement by means of Bragg–Brentano diffractometer with two Johansson curved monochromators in the parallel-beam optics geometry by using a $\text{CuK}\alpha$ radiation. From broadening of XRD diffractions peaks the size of microcrystals D were evaluated using Williamson–Hall plot [26] (annealed KGW3 sample) or line-profile shape factor [27] (KGW9, KGW7 and annealed KGW10 samples) methods. Information about the microcrystalline structure of the films was obtained from the micro-Raman spectroscopy (μRS) measured using a Renishaw Ramascope (Model 1000) equipped with a Leica microscope and a CCD detector was used. A cw Ar^+ ion laser operating at 514.5 nm was focused onto the sample surface so that a spot size typically 4–5 μm in diameter and a power density 3 kW/cm^2 were reached. The polarisation of the scattered radiation was not analysed. The morphology of the films was observed by conventional SEM at a magnification of 1000 and 4000 times with accelerating voltage of 15 kV. The films composition measurement was describe more precisely in [25]. The concentration of Nd was 0.1 at.% determined by wave dispersion X-ray (WDX) analyses [25].

Excitation spectra were measured in visible (570–600 nm) and in infrared (780–830 nm) ranges. Fluorescence spectra were taken in regions 850–950 nm (${}^4\text{F}_{3/2} \rightarrow {}^4\text{I}_{9/2}$), and 1000–1140 nm (${}^4\text{F}_{3/2} \rightarrow {}^4\text{I}_{11/2}$) and 1300–1400 nm (${}^4\text{F}_{3/2} \rightarrow {}^4\text{I}_{13/2}$) of transition of Nd^{3+} ions. For excitation an excimer (XeCl) pumped dye laser (Lumonics HD 300) and a cw Ti sapphire ring laser (Coherent) of 2 GHz resolution, pumped with an Argon laser were used in visible and infrared ranges, respectively. Fluorescence in visible range was analysed with a Hilger and Watt 1 m monochromator with a grating of 1200 grooves/mm blazed at 500 nm and detected by a cooled fast response AsGa photomultiplier (RCA 31084). The signal fed into an Ortec 9320 photon-counting system for the spectral measurement, or into a Canberra multichannel analyser for the lifetime data. In IR region fluorescence was analysed with a Jobin-Yvon H25 monochromator with a grating of 600 grooves/mm blazed at 1 μm , detected with a high sensitivity germanium photodiode (ADC 403 L) cooled to liquid nitrogen temperature. The signals was fed into a PAR lock-in amplifier and digitised. Both experimental set-ups were controlled by a computer for emission and excitation spectra.

3. Results and discussion

3.1. Structural properties (XRD and micro-Raman spectroscopy)

Composition of the films and crystalline structure was already described more in detail in our previous

work [25]. Briefly, films grown at low temperature ($T_S = 400^\circ\text{C}$) on MgO and YAP substrates were amorphous. The films prepared at 400°C on YAG substrate were partly crystalline with several small diffraction peaks. Because of their small intensities and wide width the peaks cannot be distinctly associated with KGW or other similar phase. As the T_S increased the films became crystalline for all substrates, but the crystalline structure is different for each of them. The XRD pattern of films deposited on YAP substrate consists of many small broad peaks. Due to this the determination of the crystalline structure is questionable and the presence of monoclinic α -KGW was not proved. On MgO substrate the films consist of mixing of the α -KGW and $\text{Gd}_2(\text{WO}_4)_3$ (GdW) [28] phases both crystallised in the monoclinic structure. With increasing of the temperature the growing of the GdW phase is more preferential and at $T_S = 800^\circ\text{C}$ the films became (010)-GdW textured with the presence of only minority of KGW phase mainly (011) oriented. On YAG substrate taking into account the intensities of diffraction peaks of KGW [29] the film was growing preferentially in (221) orientation, nevertheless the peaks associated to the reflections from the (010), (110) and (001) crystalline planes are also presented. The diffraction peaks are much stronger and narrower in comparison with films deposited on MgO and YAP substrates. All peaks yield very well consent with monoclinic α -KGW. For YAG substrates, no unidentified peaks or peaks corresponding to the GdW phase were observed.

Fig. 1 shows the effect of a thermal annealing at 1000°C in argon atmosphere on crystalline structure of films deposited at $T_S = 400^\circ\text{C}$ on MgO and YAG substrates (KGW3 and KGW10). The strong dependence on substrate nature is evident. The α -KGW has been clearly identified only on annealed films deposited

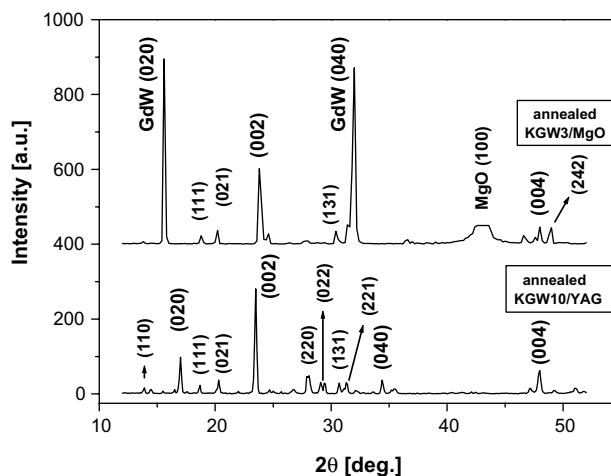


Fig. 1. XRD patterns of the films deposited at $T_S = 400^\circ\text{C}$ on MgO and YAG substrates after thermal annealing in argon atmosphere at 1000°C for 1 h.

on YAG substrate. The nearly amorphous films become polycrystalline with preferential growth in the (010) and (001) orientations. However the diffraction peaks are not as narrow as for the KGW9 sample, which was directly deposited at $T_S = 700\text{ }^\circ\text{C}$. The films deposited on MgO substrate change dramatically both composition and structure during annealing. The films become a mixture of majority GdW and minority KGW phases with crystalline planed orientated (010) and (001), respectively.

Similar influence of the substrate on the structural properties of KGW films was already presented in previous works concerning KGW films elaboration by PLD [22–25]. For example, stoichiometric polycrystalline KGW films were prepared on sapphire substrate [22,23], whereas on Si substrate mainly polycrystalline Gd_2WO_6 films were [24]. Also in our earlier work [25], small differences in composition of the films on various substrates at the same deposition conditions were observed. These differences could probably be caused by different regimes of film growth, which depend also on lattice mismatch between KGW and substrates. We assume that during the growth on the MgO substrate, the growing of monoclinic GdW phase at high T_S is preferred due to smaller lattice mismatch, like on Si substrate [27], because of the similarity of lattice parameters of (100) MgO and (100) Si crystallographic planes.

The sizes of the crystalline grains were calculated from the broadening of the XRD diffraction lines and are summarised in Table 1. The biggest crystalline grains with a size of 235 nm, were obtained for sample KGW9 deposited directly on YAG at $700\text{ }^\circ\text{C}$, while crystalline grains of the film annealed at $1000\text{ }^\circ\text{C}$ on YAG substrate were only 95 nm.

Amorphous films deposited at low T_S ($\leq 500\text{ }^\circ\text{C}$) gave no Raman signal. Only peaks coming from substrate have been observed for these films. Unfortunately films deposited on MgO substrate could not be measured, because of the strong luminescence of the MgO single crystal induced by Ar^+ laser excitation. Fig. 2 shows the micro-Raman (μR) spectra of polycrystalline KGW9 samples on YAG substrate (solid lines) and Raman spectra of polycrystalline KGW (dash grey line) [30]. The YAG substrate has no significant influence on the micro-Raman spectra of the films and rather small peaks originating from YAG, such as at 262 cm^{-1} , 372 cm^{-1} and 403 cm^{-1} , can be easily subtracted. Group-theoretical analysis predicts $17A_g + 19B_g$ Raman active vibrational modes for monoclinic (C2/c) KGW [30,31]. We were able to identify $15A_g + 9B_g$ vibrational modes. Curves (a), (b) and (c) represent typical spectra at different places on the films. As follows from the XRD measurements, the polycrystalline film (KGW9) consists of microcrystalline grains with different orientation of the main crystal axis to the substrate surface. The

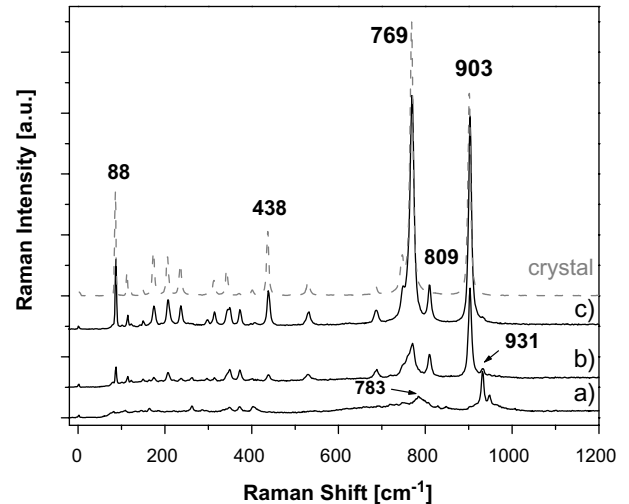


Fig. 2. Micro-Raman spectra of polycrystalline KGW9 samples on YAG substrate. Curves (a), (b) and (c) represent typical spectra at different places on the films. The dashed grey line is Raman spectra of polycrystalline KGW presented in [30].

observation of the film morphology by SEM (see below) shows with a dimension up to $5\text{ }\mu\text{m}$, which is comparable with the spot size of the exciting laser beam and so the individual microcrystals can be excited. Because of the strong anisotropy of the KGW crystal, Raman spectra depend sensitively on the mutual orientation of the laser beam, its polarization and optical axes of the crystal [4,30], the different spectra on different places of the film could be expected. Curve (a) represents probably that part of the film, where the microcrystals are small and not very well developed. Consequently, the μR spectrum is rather weak, with broad peaks. The peak at 931 cm^{-1} (B_g symmetry) dominates this spectrum, indicating that the microcrystallite probed has the orientation favourable for the appearance of the B_g modes. The shapes of curves (b) and (c) imply that these spectra were recorded on crystallites of considerably better quality and with different orientation with respect to the probing laser beam [4,31]. The spectrum of curve (c) shows that some microcrystals on the films are very well developed. This spectrum matches well with those of KGW, presented by Macalik et al. [30], both for the two strongest lines (at 769 cm^{-1} and 903 cm^{-1}) and for its broadening. Micro-Raman spectra of the KGW10 sample deposited on YAG substrate and annealed at $1000\text{ }^\circ\text{C}$ were very similar to those of the film deposited directly at $700\text{ }^\circ\text{C}$.

3.2. Morphology

The surface of amorphous films deposited at $T_S = 400\text{ }^\circ\text{C}$ on all substrates are very smooth, with minimum defects and droplets as revealed by SEM observation (Fig. 3a). With increasing T_S , the films become

polycrystalline and the microcrystals can be observed on the films surface, which becomes rougher. The size of the crystals increases with increasing T_S . Fig. 3b shows a photo at magnification 4000 times of the KGW7 sample on MgO substrate. On the surface the small randomly orientated crystals with dimension 1–2 μm are can be seen. The photo of the film deposited at YAG substrates at $T_S = 700^\circ\text{C}$ is shown on Fig. 3c. The film contains larger crystals with dimension in the region 3–5 μm . The photo in Fig. 3d shows a very special shape of mosaic structures formed by crystals smaller than 1 μm

observed for a film deposited at $T_S = 700^\circ\text{C}$ on the YAP substrate. In the case of film on the YAG substrate, after thermal annealing of amorphous films at 1000°C , the smooth surface of the films becomes rough and similar to that of films deposited directly at higher temperature. On the other hand, the film deposited on MgO substrate changed its surface morphology significantly in agreement with XRD measurement as shown in Fig. 3e. On SEM photo (Fig. 3e) we can observe two different types of crystals. Large crystals some with dimension higher than 5 μm , could be associated with

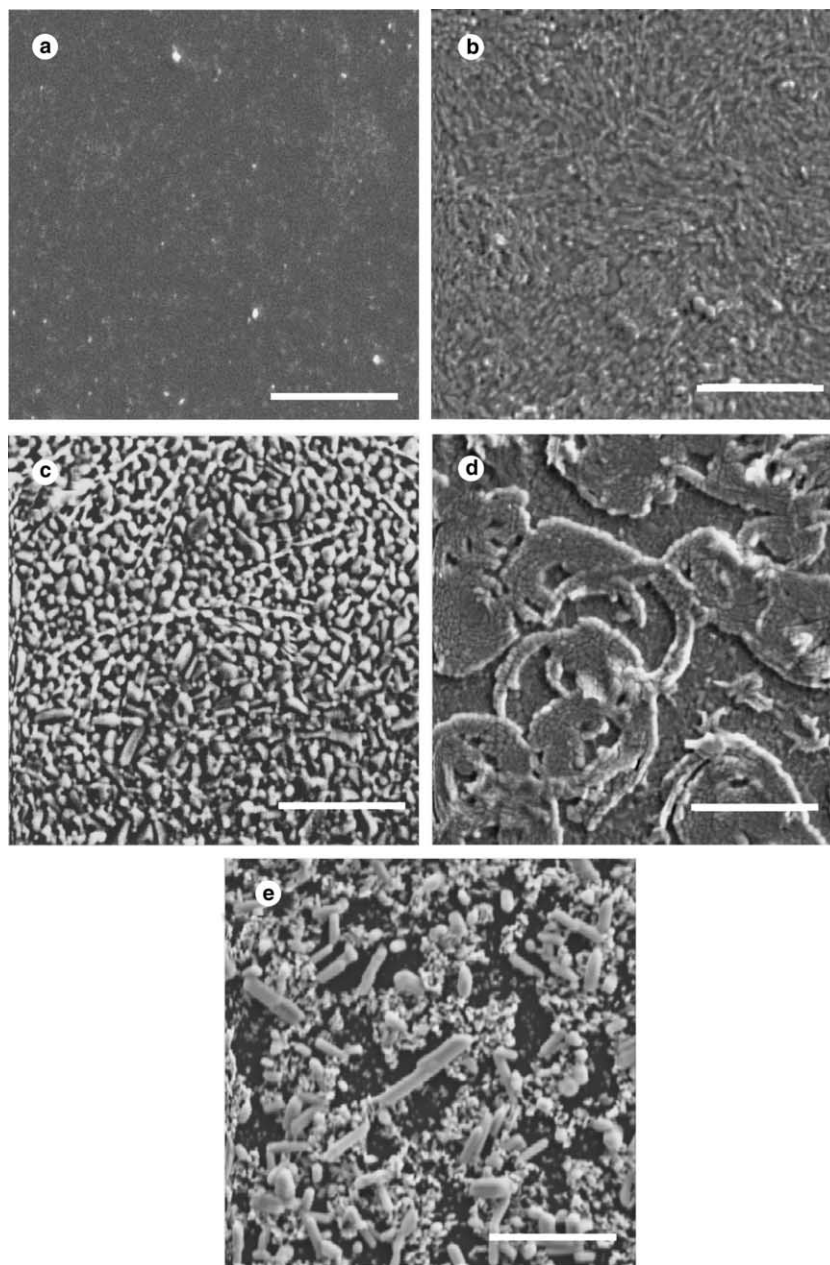


Fig. 3. The SEM photos of the films surface (a) KGW3/MgO at $T_S = 400^\circ\text{C}$, (b) KGW7/MgO at $T_S = 800^\circ\text{C}$, (c) KGW9/YAG at $T_S = 700^\circ\text{C}$, (d) KGW8/YAP at $T_S = 700^\circ\text{C}$ and (e) KGW3/MgO after thermal annealing at 1000°C in Ar atmosphere for 1 h. The magnification was 4000 times. The white line in left corner denotes 10 μm .

GdW, because of XRD peaks belonging to this phase are much narrower and stronger, and small crystals with dimension around 1 μm represent the crystalline KGW phase. The size of the microcrystals evaluated from SEM photos are summarised in Table 1. The dimensions of microcrystals determined from SEM are higher than those inferred from XRD patterns. The size calculated from XRD diffraction pattern corresponds to the dimension of zones of coherent scattering and is generally smaller than the size determined by electron or optic microscopy. This difference predicts that the crystals, which are observed by SEM, are not perfectly homogeneous and consist in smaller zones, where the crystalline planes are equidistant so that coherent scattering can occur.

3.3. Fluorescence properties

In Fig. 4–6 are presented the fluorescence spectra of the films deposited at low temperature (400 $^{\circ}\text{C}$) on MgO and YAG substrates and at high temperature (700 or 800 $^{\circ}\text{C}$) on MgO, YAG and YAP, as well as those of a film deposited at 400 $^{\circ}\text{C}$ on YAG and an-

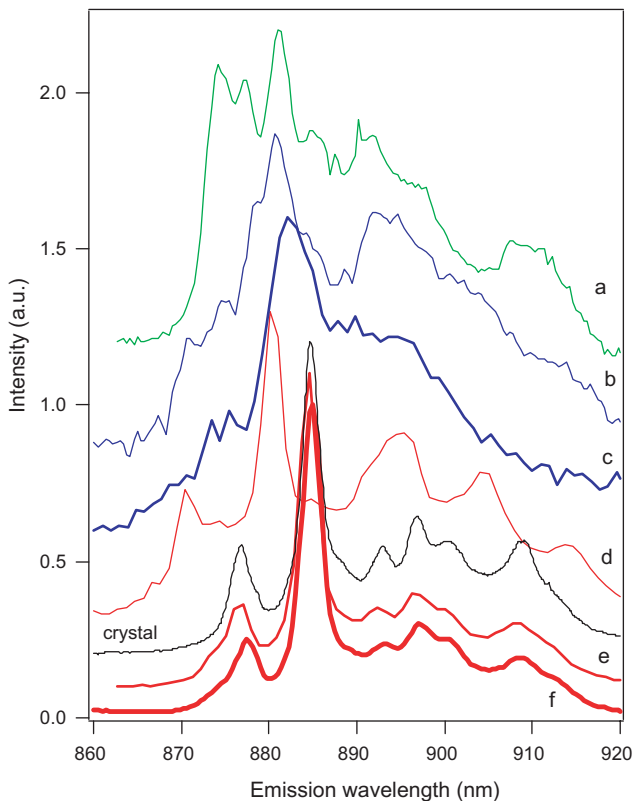


Fig. 4. ${}^4\text{F}_{3/2} \rightarrow {}^4\text{I}_{9/2}$ fluorescence spectra of films deposited (a) on YAP at 700 $^{\circ}\text{C}$, (b) on MgO at 400 $^{\circ}\text{C}$, (c) on MgO at 800 $^{\circ}\text{C}$, (d) on YAG at 400 $^{\circ}\text{C}$, (e) on YAG at 700 $^{\circ}\text{C}$, (f) on YAG annealed at 1000 $^{\circ}\text{C}$. The fluorescence spectrum of single crystal is also added for comparison [6]. Excitation wavelength: 810 nm. The curves were normalised and shifted by an arbitrary factor for clarity improvement.

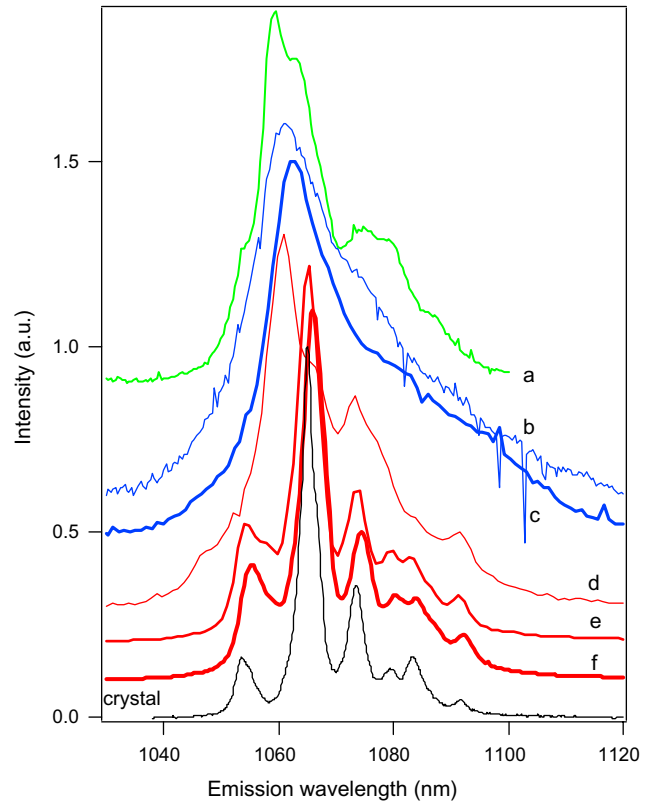


Fig. 5. ${}^4\text{F}_{3/2} \rightarrow {}^4\text{I}_{11/2}$ fluorescence spectra of films deposited (a) on YAP at 700 $^{\circ}\text{C}$, (b) on MgO at 400 $^{\circ}\text{C}$, (c) on MgO at 800 $^{\circ}\text{C}$, (d) on YAG at 400 $^{\circ}\text{C}$, (e) on YAG at 700 $^{\circ}\text{C}$, (f) on YAG annealed at 1000 $^{\circ}\text{C}$. The fluorescence spectrum of single crystal is also added for comparison [6]. Excitation wavelength: 810 nm. The curves were normalised and shifted by an arbitrary factor for clarity improvement.

nealed at 1000 $^{\circ}\text{C}$. The spectra of a Nd:KGW single crystal [5] are included in the figures for comparison. The fluorescence range is that of the three main transitions of interest for laser applications: ${}^4\text{F}_{3/2} \rightarrow {}^4\text{I}_{9/2}$, ${}^4\text{F}_{3/2} \rightarrow {}^4\text{I}_{11/2}$ and ${}^4\text{F}_{3/2} \rightarrow {}^4\text{I}_{13/2}$. For all these spectra, the excitation wavelength is 810 nm, which is that of the main absorption line from the ground state ${}^4\text{I}_{9/2}$ to the multiplets group ${}^4\text{F}_{5/2} - {}^2\text{H}_{9/2}$ for Nd:KGW single crystal [5]. Only the spectra of the films grown on YAG substrate, or deposited at 700 $^{\circ}\text{C}$ or annealed at 1000 $^{\circ}\text{C}$, which have indeed the right crystalline phase according to X-ray diffraction, are similar to those of a Nd:KGW single crystal. We already reported some of these spectra in [24] where the influence of the substrate nature was shortly mentioned. The emission spectra of the films deposited on MgO and YAP or on YAG at 400 $^{\circ}\text{C}$, which are amorphous or which contains, in addition, other crystalline phase, according to X ray diffraction, are indeed very different. The excitation spectra recorded monitoring the 1065 nm emission, which is the main emission line for the Nd:KGW single crystal, were registered in the ${}^4\text{I}_{9/2} \rightarrow {}^4\text{F}_{5/2} - {}^2\text{H}_{9/2}$ transition range and depend on substrate nature and deposition temperature

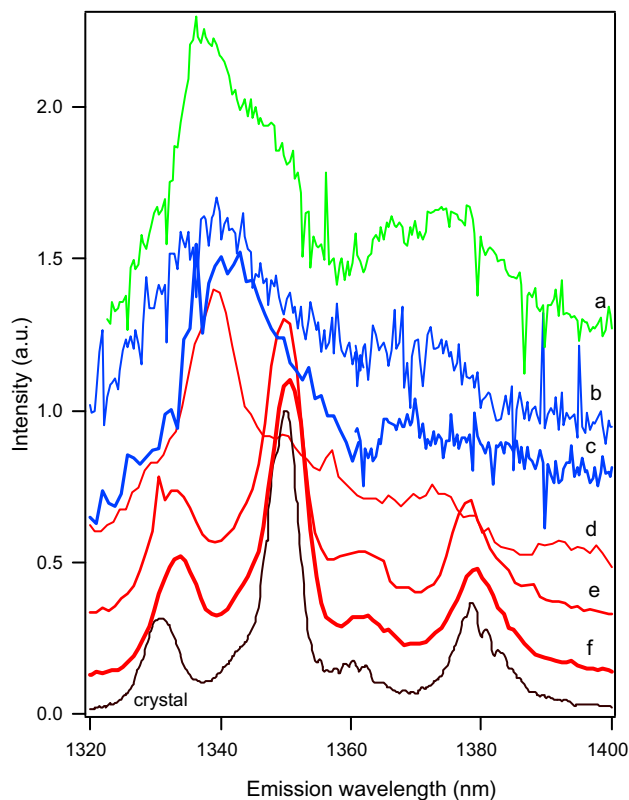


Fig. 6. ${}^4F_{3/2} \rightarrow {}^4I_{13/2}$ fluorescence spectra of films deposited (a) on YAP at 700 °C, (b) on MgO at 400 °C, (c) on MgO at 800 °C, (d) on YAG at 400 °C, (e) on YAG at 700 °C, (f) on YAG annealed at 1000 °C. The fluorescence spectrum of single crystal is also added for comparison [6]. Excitation wavelength: 810 nm. The curves were normalised and shifted by an arbitrary factor for clarity improvement.

as well (Fig. 7). Only for the films deposited on YAG at 700 °C or annealed at 1000 °C, a line at 810 nm dominates the spectrum, as for the KGW single crystal [5].

3.3.1. Films deposited on MgO substrate

The film deposited on MgO at 400 °C is amorphous, according to X-ray diffraction, and the spectra are constituted of unresolved, broad bands peaking at 880 nm, 1.06 μm and 1.34 μm for the three main emissions and 807 nm for the excitation. These spectra are characteristic of the disordered environment of Nd^{3+} ions in an amorphous matrix. The increase in the deposition temperature to 800 °C leads to a decrease in the width of the bands and a shift of the wavelengths of the band maxima towards those of Nd:KGW, but no narrower features are observed although KGW and GdW crystalline phases were detected by X-ray diffraction. Fluorescence indicates thus that the sites available in these compounds and occupied by the Nd^{3+} ions are strongly disordered and distorted. Furthermore the fluorescence intensity is very weak (about two orders of magnitude less than for the film which has the right KGW structure).

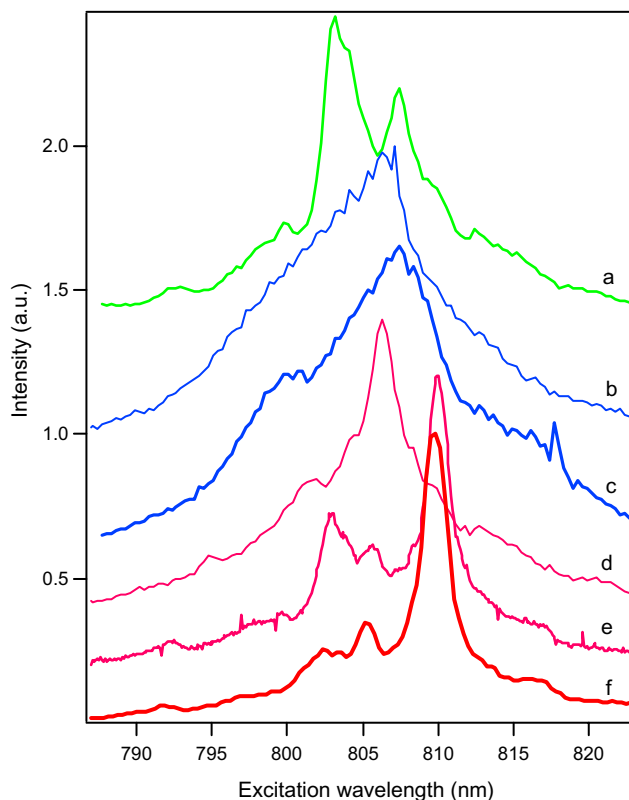


Fig. 7. ${}^4I_{9/2} \rightarrow {}^4F_{5/2} - {}^2H_{9/2}$ excitation spectra of the 1065 nm emission for films deposited (a) on YAP at 700 °C, (b) on MgO at 400 °C, (c) on MgO at 800 °C, (d) on YAG at 400 °C, (e) on YAG at 700 °C, (f) on YAG annealed at 1000 °C. The curves were normalised and shifted by an arbitrary factor for clarity improvement.

3.3.2. Film deposited on YAP substrate

The fluorescence of the film deposited at 700 °C on YAP substrate, which is poorly crystallised, has a very weak intensity too but the spectra are different from those of the films deposited on MgO. They are constituted of broad bands, which are shifted relative to those of the amorphous films deposited on MgO and show, in addition, narrower features indicative of a partial crystallisation. The wavelengths of these lines, however, do not correspond to those of Nd:KGW. This is in agreement with the fact that the X-ray diffraction peaks could not be attributed to KGW nor to any other phase, such as GdW. **From RBS experiment [24], it was clear that the interface between the YAP substrate and the film was strongly blurred by interdiffusion. This could probably explain the contribution to fluorescence and X-ray diffraction of amorphous and still non-identified crystalline phases.**

3.3.3. Films deposited on YAG substrate

The film deposited on YAG substrate at 400 °C, although nearly amorphous, according to X-ray diffraction, has emission and excitation spectra which show well-resolved lines, superimposed over a broad component.

The positions of all these lines, in particular those of the main lines in the emission (880.5 nm, 1060.8 nm and 1339 nm) and excitation spectra (806.3 nm), are different, however, from those of the Nd:KGW spectra. We were not able to determine to which compound these spectra could be attributed from the literature data.

For the film deposited at 700 °C or for the film deposited at 400 °C and annealed at 1000 °C, which are the only ones with pure KGW phase according to X-ray diffraction, the spectra are very similar to those of the single crystal. These two films show, however, two differences relative to the crystal. First, the films spectra have slightly broadened lines in comparison to those of the single crystal. For example, the FWHM for the main line of the ${}^4F_{3/2} \rightarrow {}^4I_{11/2}$ transition at 1065.4 nm is evaluated as 5.1 nm instead of 3.4 nm [5]. As a consequence, a lower resolution of the different Stark components of the transitions is observed. This inhomogeneous broadening is due to the imperfect crystalline structure of the film and to the small size of the crystallites, already attested by the broadening of the X-ray diffraction lines. For the annealed film, in addition, a slight shift of the lines and modification in multiplets splitting indicate that the distribution of crystalline field, inducing the inhomogeneous broadening, is slightly different for the two films. A second difference is the existence of a bump at about 873 nm in the ${}^4F_{3/2} \rightarrow {}^4I_{9/2}$ transition range, which could be indicative of the presence of another phase in addition to the KGW phase. In order to observe this additional line more easily, we registered the spectra of the ${}^4F_{3/2} \rightarrow {}^4I_{9/2}$ transition using excitation into the ${}^4I_{9/2} \rightarrow {}^4G_{5/2} - {}^2G_{7/2}$ transition at about 590 nm. With the corresponding experimental set-up equipped with a pulsed laser and a photomultiplier, we took advantage of the better sensitivity and of the possibility to record the fluorescence decays of the different components. Due to the photomultiplier cut-off, the spectra are restricted to wavelengths lower than 900 nm that is to the transitions to the lowest Stark sub-level of the ${}^4I_{9/2}$ multiplet. The emission spectra are given in Fig. 8. In addition to the two first lines of the usual emission of Nd³⁺ ions in KGW at 876 and 884 nm (${}^4F_{3/2}(2) \rightarrow {}^4I_{9/2}(1)$ and ${}^4F_{3/2}(1) \rightarrow {}^4I_{9/2}(1)$ transitions), an additional line is clearly observed at 874 nm. This additional line is associated to a second line at 871 nm, evidenced for the annealed film for which the intensity of these additional features is stronger. The excitation spectra of the regular line at 884 nm and of the additional line at 874 nm are different, the main excitation line being located at 575 nm and 578 nm respectively. The fluorescence decays of both lines are exponential but with different time constant (Fig. 9). The regular fluorescence lifetime is 110 μs as for the KGW crystal and 130 μs for the additional line. The identification of the minority phase, however, is not possible at the present time.

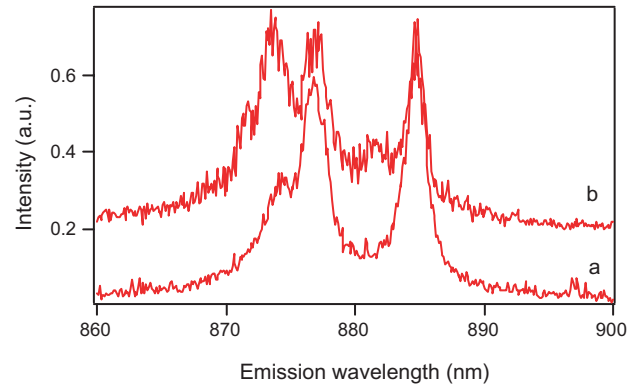


Fig. 8. ${}^4F_{3/2}$ emission spectra to the ground sub-level of ${}^4I_{9/2}$ for films deposited (a) on YAG at 700 °C ($\lambda_{exc} = 578$ nm), (b) on YAG annealed at 1000 °C ($\lambda_{exc} = 575$ nm).

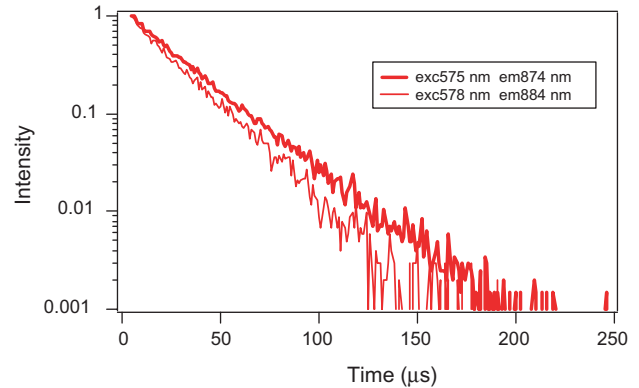


Fig. 9. ${}^4F_{3/2}$ fluorescence decays of the two Nd³⁺ sites in a KGW film deposited on YAG at 400 °C and annealed at 1000 °C.

4. Conclusion

We have reported the growing of Nd doped KGW films grown on (100) MgO, (100) YAP and (100) YAG substrates by PLD technique. The films deposited at substrate temperature T_S lower than 500 °C were nearly amorphous. With increasing of T_S , the films became crystalline, but there were large differences between the substrates used. The monoclinic α -KGW was deposited only on YAG substrate at high T_S (700 °C). The crystals have an average size of about 235 nm calculated from XRD pattern and form aggregates of 3–5 μm size as evaluated from the SEM photos. Nevertheless fluorescence measurements showed the presence of some additional minority phase, which could not be observed by the less sensitive XRD technique, probably due to the overlapping of diffraction lines with much stronger peaks belonging to α -KGW. The subsequent thermal annealing of amorphous films deposited at $T_S = 400$ °C in Ar atmosphere at a temper-

ature of 1000 °C significantly changes the structure of films deposited on MgO substrate. The films were mainly (010) Gd₂(WO₄)₃ with crystalline grains up to 10 μm observed by SEM, whereas the monoclinic α-KGW phase was obtained for the film made on YAG substrate as for the film directly deposited at high T_S. The μR spectra of film deposited on YAG substrate corresponded with α-KGW single crystal and confirmed the microcrystalline structure of films with different orientation of the microcrystals relative to the substrate surface. This, together with the anisotropy of KGW itself, is responsible for the different structure of the μR spectra obtained at different places of the films. The surfaces of films deposited at lower T_S were smooth with minimum defects. With increasing T_S, as films crystallisation occurred, the surface became rough.

Fluorescence properties corresponding to the transitions from the ⁴F_{3/2} doublet to the ⁴I_{9/2}, ⁴I_{11/2} and ⁴I_{13/2} multiplets, at about 890 nm, 1.06 μm and 1.3 μm, were studied. They bring new information about the structure of the film at the scale of the Nd³⁺ ions environment. For the films deposited on MgO substrate, whatever amorphous or crystallised into KGd(WO₄)₂ or Gd₂(WO₄)₃ phases, the Nd³⁺ fluorescence spectra are constituted of unresolved broad bands indicative of a strongly disordered environment, insensitive to the global film structure. For the films deposited on YAP substrate, the fluorescence spectra, constituted of narrow features superimposed on broad bands, show a partial crystallisation as does X-ray diffraction, although no identification of the crystalline compound was possible. Only for the films deposited on YAG substrate at high temperature (700 °C) or after annealing at 1000 °C, are the correct fluorescence spectra of Nd:KGW obtained, with the same line positions (main transition at 1065.4 nm) and life time (110 μs) as for single crystalline Nd:KGW. Slight broadening of the lines and the presence of weak additional lines are indicative of crystallisation imperfection probably due to the small size of the crystallites and of a minority phase.

From our study it follows, that polycrystalline textured Nd:KGW films have been prepared successfully on YAG substrate at high deposition temperature (700 °C) and high oxygen pressure (20 Pa), with fluorescence properties close to those of single crystal. For planar waveguide laser applications, further experiments should involve improvement of the deposition conditions in order to grow smoother and better crystallised Nd:KGW films without any minority phase.

Acknowledgments

The work was supported by the project LN00A015 of the Ministry of Education of the Czech Republic and by

Grant Agency ASCR project no. A1010110/01. Jan Lančok would like to thank for support to post-doc grant GAČR GP106/01/D017. Jindrich Chval and V. Studnička are thanked for SEM photos and XRD measurement, respectively.

References

- [1] A.A. Kaminskii, P.V. Klestov, A.A. Pavlyuk, *Phys. Status Solidi A* 5 (1971) K79.
- [2] A.A. Kaminskii, J.B. Gruber, S.N. Bagaev, K. Ueda, U. Hommerich, J.T. Seo, D. Temple, B. Zandi, A.A. Kornienko, E.B. Dunina, A.A. Pavlyuk, R.F. Klevtsova, F.A. Kuznetsov, *Phys. Rev. B* 65 (2002) 6512.
- [3] J. Viscakas, I. Mochalov, A. Mikhailov, R. Klestova, A. Liubino, *Liet. Fiz. Rinkiny* 28 (1988) 224, ICDD N. 80-455.
- [4] I.V. Mochalov, *Opt. Eng.* 36 (1997) 1660.
- [5] M.C. Pujol, M. Rico, C. Zaldo, R. Sole, V. Nikolov, X. Solans, M. Aguilo, F. Diaz, *Appl. Phys. B* 68 (1999) 187.
- [6] R. Moncorge, B. Chambon, J.Y. Rivoire, N. Garnier, E. Descroix, P. Laporte, H. Guillet, S. Roy, J. Mareschal, D. Pelenc, J. Doury, P. Farge, *Opt. Mater.* 8 (1997) 109.
- [7] A.A. Demidovich, A.P. Shkadarevich, M.B. Danailov, P. Apai, T. Gasmi, V.P. Gribkovskii, A.N. Kuzmin, G.I. Ryabtsev, L.E. Batay, *Appl. Phys. B* 67 (1998) 11.
- [8] Y. Kalisky, L. Kravchik, C. Labbe, *Opt. Commun.* 189 (2001) 113.
- [9] A.A. Kaminskii, A.A. Pavlyuk, I.F. Balashov, V.A. Berenberg, V.V. Lyubchenko, V.A. Fedorov, T.I. Butaeva, L.I. Bobovich, *IZV. Akad. Nauk SSSR Neorgan. Mater.* 13 (1977) 1541.
- [10] A.V. Kuleshov, A.A. Lagatsky, A.V. Podlipenski, V.P. Mikchailov, G. Huber, *Opt. Lett.* 22 (1997) 1317.
- [11] F. Brunner, G.J. Spuhler, J. Aus der Au, L. Krainer, F. Morier-Genoud, R. Paschotta, N. Lichtenstein, S. Weiss, C. Harder, A.A. Lagatsky, A. Abdolvand, N.V. Kuleshov, U. Keller, *Opt. Lett.* 25 (2000) 1119.
- [12] M.C. Pujol, J. Massons, M. Aguilo, F. Diaz, M. Rico, C. Zaldo, *IEEE J. Quant. Electron.* 38 (2002) 93.
- [13] A.A. Kaminskii, S.N. Bagaev, A.A. Pavlyuk, *Phys. Status Solidi A* 151 (1995) K53.
- [14] C. Zaldo, M. Rico, C. Cascales, M.C. Pujol, J. Massons, M. Aguilo, F. Diaz, P. Porcher, *J. Phys.-Condens. Matter* 12 (2000) 8531.
- [15] A.A. Kaminskii, L. Li, A.V. Butashin, V.S. Mironov, A.A. Pavlyuk, S.N. Bagayev, K. Ueda, *Jpn. J. Appl. Phys.* 36 (1997) L107.
- [16] R. Solé, V. Nikolov, X. Ruiz, J. Gavalda, X. Solans, M. Aguilo, F. Diaz, *J. Cryst. Growth* 169 (1996) 600.
- [17] C.J. Flood, D.R. Walker, H.M. van Driel, *Appl. Phys. B* 60 (1995) 309.
- [18] M.B. Korzinski, Ph. Lecoeur, B. Mercey, P. Camy, J.L. Doualan, *Appl. Phys. Lett.* 78 (2001) 1210.
- [19] J. Lančok, M. Jelinek, C. Grivas, F. Flory, E. Lebrasseur, C. Garapon, *Thin Solid Films* 346 (1999) 284.
- [20] D.S. Gill, A.A. Anderson, R.W. Eason, T.J. Warburton, D.P. Shepherd, *Appl. Phys. Lett.* 69 (1996) 10.
- [21] A.A. Anderson, R.W. Eason, L.M.B. Hickey, M. Jelinek, C. Grivas, D.S. Gill, N.A. Vainos, *Opt. Lett.* 22 (1997) 1556.
- [22] P.A. Atanasov, R.I. Tomov, J. Perriere, R.W. Eason, N. Vainos, A. Klini, A. Zherikhin, E. Millon, *Appl. Phys. Lett.* 76 (2000) 2490.
- [23] T. Okato, P.A. Atanasov, M. Obara, *Appl. Phys. A* 77 (2003) 395.

- [24] P.A. Atanasov, A. Perea, M. Jimenez de Castro, J.A. Chaos, J. Gonzalo, C.N. Afonso, J. Perriere, *Appl. Phys. A* 74 (2002) 109.
- [25] M. Jelinek, J. Lančok, M. Pavelka, P.A. Atanasov, A. Macková, F. Flory, C. Garapon, *Appl. Phys. A* 74 (2002) 481.
- [26] H.P. Klug, L.E. Alexander, *X-ray Diffraction Procedures for Polycrystalline and Amorphous Materials*, 2nd ed., John Wiley & Sons, New York, 1974.
- [27] Th.H. De Keijser, J.I. Langford, E.J. Mittemeijer, A.B.P. Vogels, *J. Appl. Cryst.* 15 (1982) 308.
- [28] F. McCarthy, Penn. State University, University Park, PA, USA, Private Communication, PDF ICDD-PDF2, card number 23-1076, Release 2000 database.
- [29] PDF ICDD-PDF2, cards numbers 45-55 and 80-455, Release 2000 database.
- [30] L. Macalik, J. Hanuza, A.A. Kaminskii, *J. Raman Spectrosc.* 33 (2002) 92.
- [31] Yu.K. Voronko, A.A. Sobol, S.N. Ushakov, L.I. Tsybal, *Inorg. Mater.* 36 (2000) 947.